Ceramics International **22** (1996) 287–293

0272-8842(95)00105-0
0272-8842/96/$15.00

Thermomechanical and Microstructural Evaluation of High Temperature Sintered (Mg, Mg–Ti)–PSZ

Parvati Ramaswamy, B. H. Narayana & S. Vynatheya

Materials Technology Division, Central Power Research Institute, P.B.No.9401, Bangalore 560 094, India

(Received 14 April 1995; accepted 21 June 1995)

Abstract: The sintering of (Mg, Mg–Ti)–PSZ up to 1700°C and the attendant changes in the thermal shock resistance after quenching from various temperatures have been studied. The effect has also been quantified in terms of retained bend strength after thermal cycling from four different temperatures in the range of 400°C and 1000°C to room temperature. Thermal cycling of the specimens which are sintered at 1500°C and aged at 1150°C leads to growth of Ti-rich whisker and coral-like features isostructural with cubic-ZrO_2, and these are the main contribution to the improved thermal shock resistance. Sintering at higher temperatures and thermal cycling result in markedly different precipitate morphologies because of the presence of TiO_2.

1 INTRODUCTION

The thermo-mechanical properties of zirconia (monoclinic ZrO_2) are improved by small additions of dopants such as CaO, MgO, Y_2O_3, etc., by partially stabilizing to a defect fluorite cubic structure plus monoclinic and/or tetragonal zirconia phases.[1,2] The extent of this stabilization in such a material (known as partially stabilized zirconia [PSZ]) is further controlled by additives like TiO_2[3] and Al_2O_3[4] and also by suitable thermal treatments.

The thermal shock behaviour of these materials has been a subject of study by various investigators.[4,5] While PSZ has been known to possess improved thermal shock resistance (TSR) over unstabilized ZrO_2, further improvements in PSZ by employing destabilization techniques were reported of late.[3] Another technique for improving the TSR of Mg–PSZ through ageing at the sub-eutectoid temperature of this system (e.g. 1100°C) was reported by Hannink and Garvie.[6] The marked improvement was attributed to the occurrence of a type of solid state reaction during ageing, resulting in the presence of microdomains of the fluorite related superstructure $Mg_2Zr_5O_{12}$.

The authors have reported excellent thermal shock resistance properties for titania destabilized Mg–PSZ sintered at 1500°C for 4 h.[3] Evaluation consisted of quenching ceramic bars several times (50) between 1150°C and water at room temperature.

Ageing these materials at 1150°C for long duration (3–50 h) has also resulted in improved TSR and bend strength.[7] The strength retained in these materials when aged at 1150°C for 25 h and subsequently quenched from various temperatures between room temperature (RT) and 1000°C, varies between 40 and 65% of the original strength.

It is well known that the conventional temperature of sintering Mg–PSZ is around 1700°C.[8] Keeping this in view, our Mg–Ti–PSZ system is also sintered at temperatures above 1500°C, up to 1700°C. The ageing response of this system when aged around the sub-eutectoid temperature and the thermo-mechanical behaviour is discussed hereafter.

2 EXPERIMENTAL DETAILS

Ceramic grade zirconia, magnesia and titania (rutile) powders were employed to prepare the

Mg–PSZ and Mg–Ti–PSZ compositions. The basic composition was 10 mol% MgO/90 mol% ZrO_2, to which was added an extra 4 and 6 mol% TiO_2. Composition details are given in Table 1.

These compositions were prepared by wet ball-milling and pressed into 75 mm x 25 mm x 7 mm bars in the conventional manner, the details of which are given elsewhere.[3] These samples were sintered at 1650°C for 3 h and at 1700°C for 4 h in static air and furnace cooled by shutting off the furnace.

Ageing of the sintered bars was carried out at 1150°C for 25 h. The bend strength of these bars was measured by the three point bend method (span 50 mm).

The thermal shock properties of the as-sintered and aged samples were studied in two ways. The tests conducted were:

1. Water quench to failure : Samples were introduced into a furnace and held for 1 h at 1150°C and quenched in water at room temperature. The up and down shock cycles were repeated until the specimen failed.
2. Retained strength after air quench : The specimens were held at four different temperatures (400, 600, 800 and 1000°C) for 1 h and air quenched. The retained bend strengths of the samples were measured after subjecting them to five such thermal cycles. The above tests were carried out on seven test bars each time and the data reported here are the average values obtained from a minimum of five test specimens. The data possess a scatter not more than ±5% from the average values indicated in the relevant table and figure.

The specimens were also characterised for microstructure, chemical composition and phases by scanning electron microscopy (SEM with EDAX attachment) and X-ray diffractometry (XRD) using CuKα radiation.

3 RESULTS AND DISCUSSION

The set of samples fired both at 1650°C and 1700°C appeared to be well sintered without any deformation or visible flaws. Sintering at these two higher temperatures also yielded phases similar to those observed in the specimen sintered at 1500°C/4 h, namely cubic and monoclinic.[3] Furthermore, the extent of stabilization is at a maximum in the composition containing no titania (M_{10}) and destabilization occurs on addition of TiO_2, with the extent increasing as more TiO_2 is added.

The thermal shock damage caused due to water quench and air quench are reported in terms of the number of thermal shock cycles to failure and retained bend strength, respectively, and are discussed separately.

3.1 Water quench thermal shock

The number of thermal shock cycles to failure when cycled between 1150°C and water at RT for the specimens sintered at 1650°C and 1700°C are shown in Table 2. Results of similar samples sintered at 1500°C which had been studied by the authors are also included in the table for comparison purposes.

From Table 2, it can be seen that both the PSZ systems withstand the severe thermal shock damage but to varying degrees.

While increasing sintering temperatures from 1500°C to 1700°C through 1650°C results in marked improvement in thermal shock resistance from 3 to 17 cycles in Mg–PSZ, the effect in Mg–Ti–PSZ is deleterious.

The response of the three composition designation to ageing at 1150°C for 25 h from the point of view of TSR is dependent on the sintering temperature. When sintered at 1500°C, M_{10} does not respond to ageing at all, while Mg–Ti–PSZ ($M_{10}T_4$ and $M_{10}T_6$) respond excellently, exhibiting a marked improvement in TSR. However, a positive response of M_{10} to ageing is seen when this composition is sintered at 1650°C or 1700°C. On the other hand, the response of both $M_{10}T_4$ and

Table 1. Compositions

Designation	Basic composition (mol%)		TiO_2 added (mol%)
	ZrO_2	MgO	
M_{10}	90	10	—
$M_{10}T_4$	90	10	4
$M_{10}T_6$	90	10	6

Table 2. Number of thermal shock cycles to failure

Sintering schedule	Heat treatment	No. of thermal shock cycles to failure Composition designation (Sample dimension 75 x 25 x 7 mm)		
		M_{10}	$M_{10}T_4$	$M_{10}T_6$
(a)				
1500°C/4 h[a]	NIL	3	10	23
	1150°C/25 h	4	27	45
1650°C/3 h	NIL	10	15	15
	1150°C/25 h	20	14	11
1700°C/4 h	NIL	17	9	11
	1150°C/25 h	20	12	11

[a] Results of study reported in Ref.7.

$M_{10}T_6$, sintered at 1650°C and 1700°C, to ageing is not encouraging from TSR behaviour view point. The thermal shock behaviour of M_{10} (sintered and aged) appears to follow the trend of Mg–PSZ when sintered at high temperatures (~1700°C) as reported by Hannink and Garvie.[6] The well accepted mechanism of the occurrence of a type of solid state reaction in the presence of microdomains of the fluorite related superstructure $M9_2Zr_5O_{12}$ during sub-eutectoid ageing is probably active here. However, the negative response of Mg–Ti–PSZ compositions in their thermal shock behaviour to high temperature sintering (1700°C) and to subsequent ageing indicates the presence of some features deleterious to thermal shock resistance.

From these results it is observed that the modification of Mg–PSZ by Ti additive gives three advantages, viz. (1) sinterability at lower temperature, (2) the best TSR property within the experimental framework reported in Table 2, and (3) response to ageing of materials sintered at 1500°C is good and results in improved TSR. However, at higher sintering temperature the response even after ageing is not favourable.

3.2 Retained bend strength after air quench

The extent of damage caused by thermal shock treatment is reported in terms of loss of bend strength. The results of the extent of damage for the systems sintered at 1500°C were reported earlier.[7]

Figure 1 graphically depicts the bend strength of all three of the designated compositions sintered at 1650°C. The data included cover the samples in as-sintered condition, as-aged condition and the aged samples after quenching in air five times at four different temperatures.

Ageing the Mg–PSZ and Mg–Ti–PSZ at 1150°C for 25 h brings about significant improvements in their bend strengths over the as-sintered (at 1650°C) specimens. The improvement is very pronounced in Mg–T–PSZ. This trend in the presence of Ti was observed in these systems during their sintering at 1500°C and subsequent ageing also.[7]

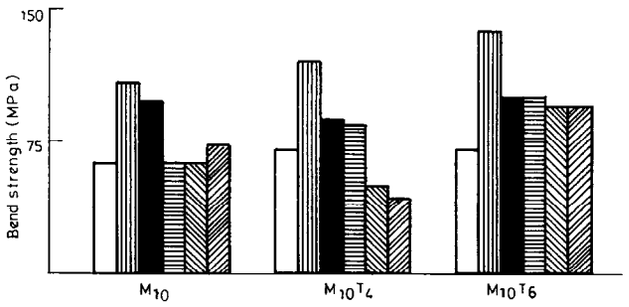

Fig. 1. Bend strength of (Mg, Mg–Ti)–PSZ. (□) as-sintered, (▥) aged, 1150°C/25 h, and quenched thermally five times at (■) 400°C RT, (▤) 600°C ⇌ RT, (▧) 800°C ⇌ RT, and (▨) 1000°C ⇌ RT.

In M_{10}, the aged samples subjected to quenching in air from 400, 600, 800 and 1000°C possessed a retained strength not lower than the strength they had in the as-sintered condition, but lower than the as-aged strength.

In the Mg–Ti–PSZ, i.e. $M_{10}T_4$ and $M_{10}T_6$, the aged samples subjected to similar quenching in air at the four temperatures, possessed a retained strength clearly higher than the strength they had in the as-sintered condition, but lower than the as-aged strength. The ability to retain higher strength is higher in the compositions with increased Ti content, viz. $M_{10}T_6$. Comparing the retained strengths of $M_{10}T_4$ and $M_{10}T_6$ quenched from 800 and 1000°C, the values for $M_{10}T_4$ are surprisingly low and there does not seem to be any obvious reason for this behaviour, which has been attributed to the not-so-obvious and unnoticeable defects in the test sample during processing itself. Scanning microscopic analysis of the fracture surfaces of these samples showed layer formation, which may originate during the process of dry pressing the ceramic powders.

The result of the retained strengths of Mg–Ti–PSZ samples sintered at 1500°C and presently at 1650°C are compared. Our earlier observations, for the specimen sintered at 1500°C, that damage due to thermal shock cycles is caused even at lower temperature differentials seems to be true in the case of sintering at 1650°C as well. However, the extent of damage caused is itself lower in the latter. In other words, resistance to such damage is improved when Mg–Ti–PSZ is sintered at 1650°C compared to 1500°C. Comparing the percentage retained strength, sintering at 1650°C allows the retention to be at least 70%, while it was in the range of 40–65% when sintered at 1500°C.

Similar strength retention in Mg–PSZ (sintered at 1700°C) has been reported by Hannink and Garvie.[6] The samples which were sub-eutectoid aged were thermally shocked between 450°C and molten aluminium at 900°C. Initial bend strength values of the order of 450 MPa have been reported in the as-aged condition by them. However, such values have not been observed in the present case. This may possibly be due to the larger dimensions of the specimen (75 x 25 x 7 mm) used by us, compared to the relatively thinner specimen (40 x 3 x 3 mm) used by Hannink and Garvie. The difference in the bulkiness of the samples increases the chances of both surface and bulk defects and flaws in the larger specimen. It may further be worth mentioning that the severity of thermal shock can

be viewed as higher in the present study. This arises out of two factors:

1. sample was thermally shocked between room temperature and 400–1000°C five times and
2. the bulkier sample can be expected to experience higher thermal stress gradients.

3.3 Microstructure

3.3.1 Sintering at 1500°C

The microstructural manifestation of these systems under starting condition of sintering at 1500°C followed by heat treatment and thermal shock have been discussed elsewhere.[9] To aid the present discussion, Fig. 2 gives the microstructure of the as-sintered M_{10}. Uniformly distributed polyhedral grains with average grain size of about 4 μm along with evenly distributed pores form the microstructural features. Thermal shock treatment does not bring about any significant microstructural changes in this composition. The $M_{10}T_4$ and $M_{10}T_6$ specimens also have similar features except that the average grain size is about 2 μm, indicating that TiO_2 acts as a grain growth inhibitor in this system.

Subjecting TiO_2-bearing sintered samples to thermal shock cycles results in a significantly different fractograph from M_{10}. While intergranular cracks in the fracture is the only development seen in M_{10} on thermal shocking, both $M_{10}T_4$ and $M_{10}T_6$ exhibit spherodised grains and growth of Ti-rich needle-like whiskers.[9] The Ti-rich whisker-like features have been found to form during thermal shock cycling between ~1100°C and RT with intermittent hold at the higher temperature. The excellent thermal shock behaviour has been attributed to this reinforcing feature in the microstructure. These features are shown in the fractograph of $M_{10}T_6$, which has been thermal shock cycled between 1150°C and water at RT to failure (Fig. 3).

The fractograph of aged samples (M_{10}, $M_{10}T_4$, $M_{10}T_6$) did not show any difference in the microstructural features as compared to the as-sintered samples. However, the aged samples behaved differently once again, when subjected to thermal shock cycles. The microstructure of such an aged $M_{10}T_6$, having undergone several thermal shock cycles, is given in Fig. 4.

Although the microstructures of as-sintered and aged Mg–Ti–PSZ are similar, they are distinctly different after thermal shock cycling. The difference is evident on comparison of Figs 3 and 4. Figure 4 shows that the well-defined needle-like shape of the whiskers (in Fig. 3) is not retained, but ageing followed by thermal shocking results in uniformly spread coral-like islands. EDAX analysis of these islands confirmed them to be Ti-rich, as was the case for the needles. The presence of uniformly spread Ti-rich islands once again substantiates their role as reinforcing features in further improving the thermal shock resistance of Mg–Ti–PSZ, as seen from Table 2. The origin of the coral-like features is not very clear. It is probable that the formation of very fine Ti-rich precipitates begins during the heat treatment schedule at 1150°C/25 h. These manifest themselves as coral-like islands during thermal shock cycling which may be entangled clusters of needle-like morphology. Thus, although the two precipitate morphologies may appear different, their reinforcing effects are similar and impart higher thermal shock resistance depending upon the distribution per unit volume.

3.3.2 Sintering at 1650°C

On sintering at 1650°C, M_{10} exhibits a different microstructure compared to the TiO_2-bearing

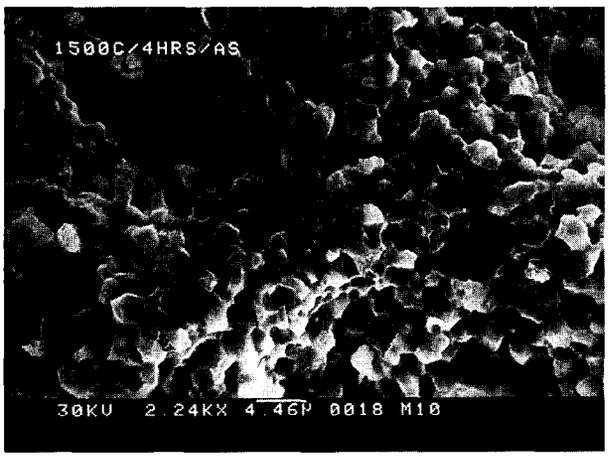

Fig. 2. SEM fractograph of M_{10}, as-sintered 1500°C/4 h.

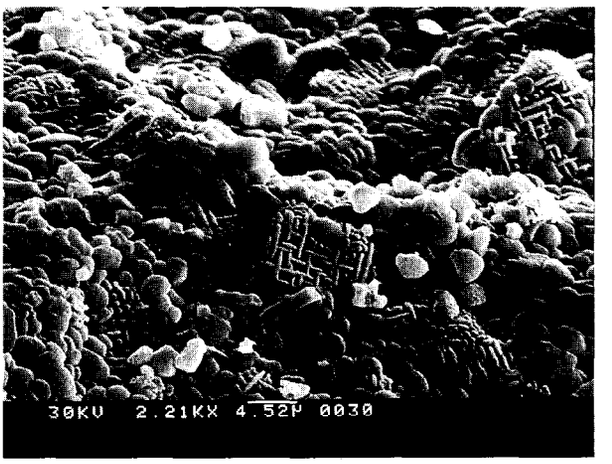

Fig. 3. SEM fractograph of sintered $M_{10}T_6$ after 20 thermal shock cycles between 1150°C and RT.

compositions. The fracture in M_{10} exhibits polyhedral grains with an apparent preferential cleavage plane (Fig. 5). The increased grain size (7–10 μm) caused by higher sintering temperature is also seen. It can be seen from Figs 5 and 6 that the microstructures of $M_{10}T_4$ and $M_{10}T_6$ are similar. Two types of grain features form the microstructure: (i) small sized (2–3 μm) polyhedral and (ii) large sized coalesced dark regions (7–10 μm) with rounded small pores. The latter are probably formed because of liquid phase sintering. The EDAX analysis confirms that both these grain features are chemically identical, consisting of Zr, Mg and Ti, as in the original composition.

Microstructural features of thermal shocked $M_{10}T_4$ are shown in Fig. 7. These consist of the tendency of the grains to round off from the polyhedral shape and the disintegration of the coalesced dark region with separating wide cracks caused by thermal shock stress. Apprarently the poor TSR of these specimens under the 1650°C sintering is due to the presence of a relatively weak phase prone to disintegrate during thermal stress cycling. Qualitative EDAX analysis of the cracked region surprisingly indicated a total absence of Ti in them. This, once again, confirms the supportive role of Ti in Mg–PSZ compositions in improvement of TSR properties. It is to be noted that the presence of Ti in these compositions, probably in the form of an oxide phase rich in Ti, with small amounts of Mg and Zr, formed isostructural with Mg–PSZ, as needle-shaped whiskers during thermal cycling is the main criteria for improved TSR behaviour. The mechanism of such a migration of Ti out of the region has not been fully studied. Furthermore, the reason why sintering Mg–Ti–PSZ at 1650°C does not promote the growth of Ti-rich whisker-like features on thermal shock cycling is not known. No special features were seen in M_{10} compositions.

As in the case of the 1500°C sintering schedule, heat treatment does not bring about any change in the microstructure. Even the microstructure of thermally shocked samples did not exhibit any difference from the thermally shocked as-sintered samples (Fig. 7).

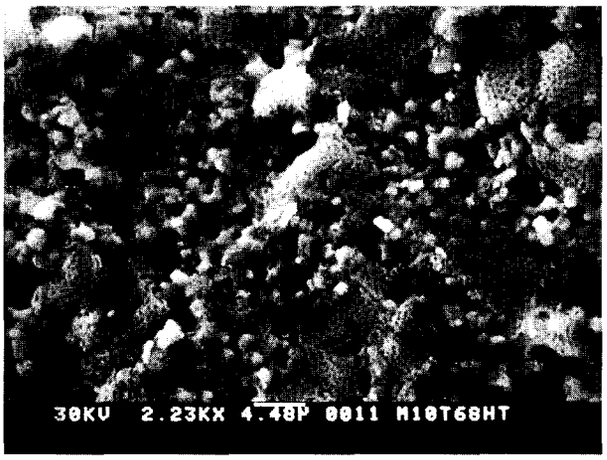

Fig. 4. SEM fractograph of aged $M_{10}T_6$ after several thermal shock cycles between 1150°C and RT.

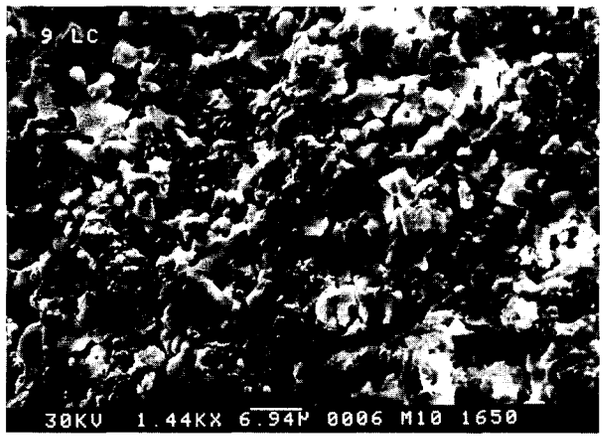

Fig. 5. SEM fractograph of M_{10}, as-sintered 1650°C/3 h.

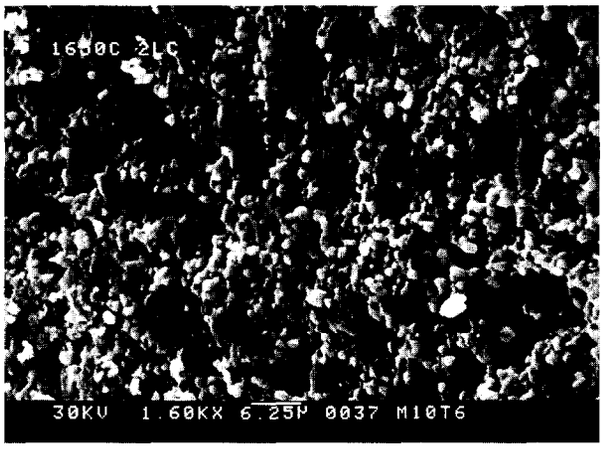

Fig. 6. SEM fractograph of $M_{10}T_6$, as-sintered 1650°C/3 h.

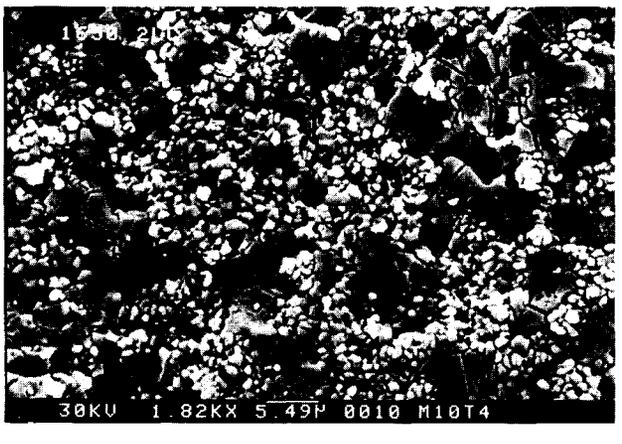

Fig. 7. SEM fractograph of thermal shocked $M_{10}T_4$ (sintering temperature 1650°C/3 h).

3.3.3 Sintering at 1700°C

Sintering the samples at 1700°C brings about dramatic changes in all three of the compositions. As-sintered fracture of M_{10} exhibits smooth extended petal-like features possessing an average grain size of 20 μm with uniformly distributed porosity (Fig. 8(a)). In contrast, $M_{10}T_6$ shows more defined polyhedral grains along with a certain degree of smudginess (Fig. 8(b)). The smudgy features, on close examination (Fig. 8(c)), reveal a woven network of needle-like whiskers. These features resemble the islands of fibrous network features of thermally shocked $M_{10}T_6$ in the 1500°C sintering schedule (Fig. 3). The thermal shock resistance of both the M_{10} and $M_{10}T_6$, however, are widely different (Table 2). This may be due to the fact that the chemical compositions of the two similar-appearing networks are entirely different. The major difference in these features is that the woven network (1700°C sintering schedule) is Zr-rich and not Ti-rich. Both the Zr-rich and Ti-rich phases may have the crystal structure of cubic-ZrO_2, since no additional peaks other than that of c-ZrO_2 and m-ZrO_2 were obtained in the X-ray diffraction pattern of all the sintered, aged and thermally cycled specimens. However, the composition of the Ti-rich needle-like whiskers (Fig. 3), as determined by the EDAX analysis, showed the Ti content to be about 95%, while in the Zr-rich features (Fig. 8(c)) it was less than 5%. According to the existing phase diagrams[10] the tetragonal and cubic phases are expected to coexist in the range 1400–1700°C. However, X-ray diffraction patterns from polished sections of the specimens showed no change in the percentage area of cubic/tetragonal peak of ZrO_2 phase, thereby confirming the absence of t-ZrO_2. This may be because the samples have not been solution annealed at any temperature in order to retain the t-ZrO_2 phase. Radford and Bratton[11] have reported that additions of TiO_2 and Al_2O_3 to calcia- and yttria-stabilized ZrO_2 promote sintering at 1460°C due to the formation of a liquid phase. The presence of liquid phase in some of our samples is also indicated in features like rounded grain morphology. Furthermore, at 1700°C, due to excessive formation of liquid phase because of sintering near the extreme side of solid solution regime (~1750°C) in the phase diagram, the Zr-rich phase may be formed as a result of fast nucleation of dendritic structures. These are undesirable from the TSR point of view. From the above experiments it becomes clear that the compositions of the whisker-like features play a more important role in improving the TSR properties of the MgO–TiO_2–ZrO_2 system. The presence of a large amount of Ti in the network (Fig. 3) brings about this significant improvement in TSR behaviour. The microstructural features in the case of $M_{10}T_4$ are very similar to $M_{10}T_6$.

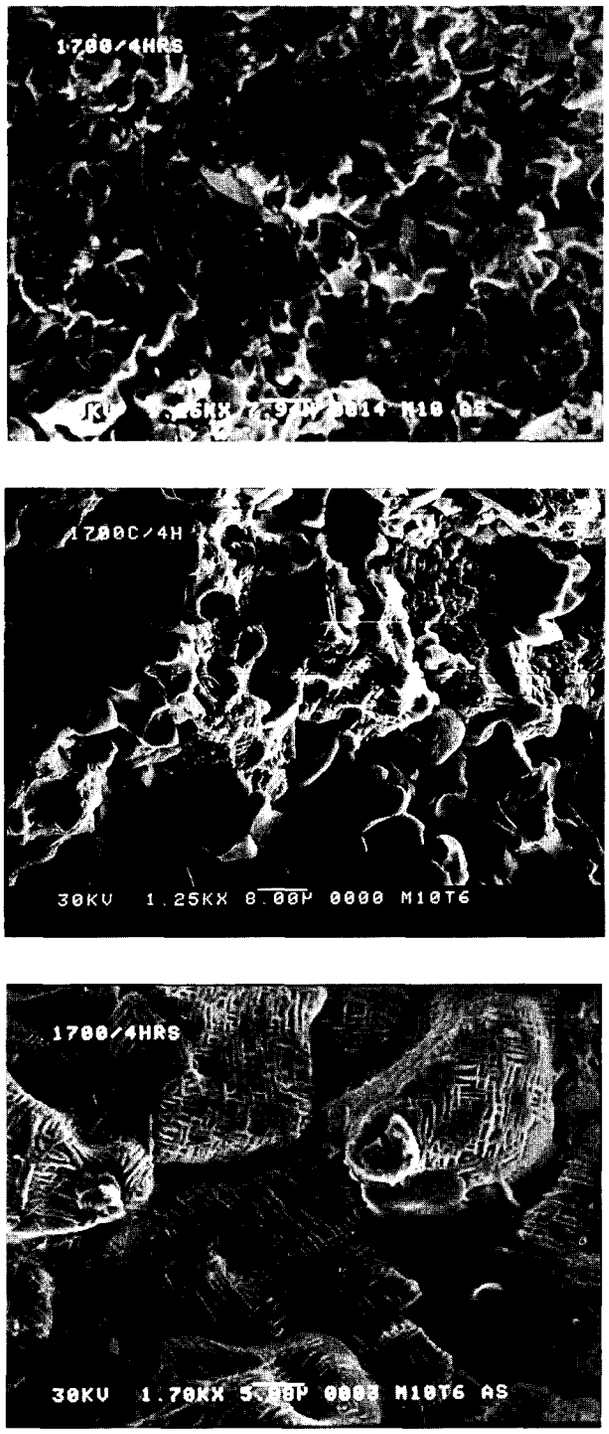

Fig. 8. SEM fractograph of as-sintered (1700°C/4 h). (a) M_{10}, (b) $M_{10}T_6$ and (c) $M_{10}T_6$ smudgy features.

Subjecting the sintered samples to thermal shock cycles, the M_{10} composition showed no change in its microstructure and $M_{10}T_6$ showed a wider spread of smudgy features almost engulfing the grains (Fig. 9). The structure is more porous.

Both heat treatment and subsequent thermal shocking did not bring about any observable changes in the microstructure of M_{10}. $M_{10}T_6$ on

Fig. 9. SEM fractograph of thermal shocked $M_{10}T_6$ (sintering temperature 1700°C/4 h).

heat treatment itself develops microstructure similar to the one shown in Fig. 9. Thermal shocking introduces cracks, but the microstructural features are retained.

4 CONCLUSIONS

The Mg–Ti–PSZ system, sintered at 1500, 1650 and 1700°C followed by ageing at 1150°C, exhibited the following properties.

1. The system possesses excellent thermal shock resistance at the 1500°C/1150°C sintering/ageing schedule. Growth of Ti-rich whisker-like features during thermal cycling reinforces the ceramic and improves the TSR behaviour.
2. Sintering at higher temperatures and ageing is detrimental from the TSR point of view. This results in rejection of Ti from Mg–Ti–PSZ to give a microstructure of either Ti-devoid phase or Zr-rich fibrous network.
3. Sintering at 1650°C and subsequent ageing allows the retention of about 70% of its as-aged bend strength until after a few thermal shock cycles at temperature differentials of ~975°C.

ACKNOWLEDGEMENT

The authors thank the CPRI management for permission to publish this paper.

REFERENCES

1. GRAIN, C., Phase relations in ZrO_2–MgO system. *J. Am. Ceram. Soc.*, **50**(6) (1967) 288.
2. GUPTA, T. K., BECHTOLD, J. H., KUZNICKI, R. C., CADOFF, L. H. & ROSSING, B. R., Stabilization of tetragonal phase in polycrystalline zirconia. *J. Mater. Sci.*, **12** (1977) 2421.
3. KRISHNAMOORTHY, P. R., PARVATI, RAMASWAMY & NARAYANA, B. H., Thermal shock behaviour of titania destabilized Mg–PSZ. *Ceram. Int.*, **16** (1990) 129.
4. ANANTHAPADMANABHAN, P. V., MENON, S. B., VENKATARAMANI, N. & ROHATGI, V. K., Thermal shock behaviour of destabilized zirconia. *Ceram. Int.*, **12** (1986) 107.
5. KARAULOV, A. G., GREBENYOK, A. A. & RUDYAK, N., Effect of phase composition of zirconium dioxide on spalling resistance. *IZV Akad. Nauk SSSR Neorg. Mater.*, **3**(6) (1967) 1101.
6. HANNINK, R. H. J. & GARVIE, R. C., Subeutectoid aged Mg–PSZ alloy with enhanced thermal up-shock resistance. *J. Mater. Sci.*, **17** (1982) 2637.
7. KRISHNAMOORTHY, P. R., PARVATI, RAMASWAMY & NARAYANA, B. H., Thermal shock and bend strength properties of the Mg–Ti-partially stabilized zirconia system. *J. Mater. Sci. Lett.*, **10** (1991) 464.
8. HANNINK, R. H. J., Microstructural development of sub-eutectoid aged MgO–ZrO_2 alloys. *J. Mater. Sci.*, **18** (1983) 457.
9. KRISHNAMOORTHY, P. R., PARVATI, RAMASWAMY & NARAYANA, B. H., Microstructural developments in Mg–Ti–PSZ systems. *J. Mater. Sci.*, **27** (1992) 1016.
10. COUGHANOUR, L. W., ROTH, R. S., MARZULLO, S. & SENN, F. E., Solid-state reactions and dielectric properties in the systems magnesia–zirconia–titania and lime–zirconia–titania. *J. Res. Nat. Bur-stand. (US)*, **54**(4) (1955) 191.
11. RADFORD, K. C. & BRATTON, R. J., Zirconia electrolyte cells. *J. Mater. Sci.*, **14**(1) (1979) 59.